J. Fluid Mech. (1977), *vol.* 82, *part* 2, *pp.* 349–369
Printed in Great Britain

A numerical model of the air flow above water waves. Part 2

By P. R. GENT

Department of Oceanography, University of Southampton, England†

(Received 27 October 1976 and in revised form 8 February 1977)

Further results from the nonlinear numerical model of the air flow in a deep turbulent boundary layer above water waves described in Gent & Taylor (1976) are presented. The results are calculated with the surface roughness z_0 both constant and varying with position along the wave. With the form used when z_0 varies, the fractional rate $|\zeta|$ of energy transfer per radian advance in phase due to the working of the pressure forces is larger than for z_0 constant both when the transfer is from wind to waves and when it is from waves to wind. The latter case occurs when the waves are travelling faster than, or against, the wind. The energy transfer rates are compared with other theoretical predictions and with recent field observations.

1. Introduction

In a previous paper (Gent & Taylor 1976, hereafter referred to as G & T), a nonlinear turbulent numerical model was proposed for the steady air flow above an infinite train of monochromatic two-dimensional waves. It was shown how nonlinear effects could become important as the wave amplitude increased and that the assumption of linearization in terms of the maximum wave slope ak used in the previous inviscid theory of Miles (1957, 1959) and the previous turbulent theories of Townsend (1972) and Long (1971) is valid only for $ak < 0{\cdot}05$. G & T also showed that the fractional rate ζ of energy input per radian advance in phase decreased with increasing wave amplitude. For constant surface roughness z_0 the predicted values of ζ, at small ak, were in close agreement with the predictions of the linear theories, which, surprisingly, are all very similar. Computations were also made in which z_0 was allowed to vary with position along the wave, however, to try to model the concentration of smaller gravity and capillary waves just forward of the wave crest; see Longuet-Higgins (1969*a*) and Keller & Wright (1975). In this case, if the variation in z_0 was half its mean value, the predicted values of ζ could be increased by a factor of between two and three for small amplitude waves. This brings ζ more into line with the laboratory work of Shemdin (1969) and the field measurements of Elliott (1972). Other field experiments by Dobson (1971*a*) and Snyder (1974) gave larger and smaller values of ζ respectively.

The present paper reports more results from the numerical model described in G & T but in different regions of parameter space. First, two series of runs with increasing amplitude are presented to highlight the nonlinear effects of the change in form and phase of the pressure and stress fields. In G & T, U_5/c was varied by keeping the phase speed c, or equivalently the wavelength, of the wave constant and altering the speed

† Present address: National Center for Atmospheric Research, Boulder, Colorado 80307.

U_5 of the wind at 5 m. In the present paper U_5 is kept constant while the wavelength of the wave is varied. These runs are compared and contrasted with the results in G & T in the range of U_5/c where energy is transferred from wind to waves. Further predictions are then presented where the energy transfer due to the pressure field is from the waves to the wind. This situation occurs when waves travel either faster than or against the wind. Finally, when the waves and wind are in the same direction, the possibility is explored of being able to predict whether the energy transfer due to the pressure field is to or from the waves, given their wavelength and the wind speed U_5. This also leads to predictions of the variations in the value of U_5/c when the direction of energy transfer changes.

2. The numerical model

The numerical model is exactly that described in detail in G & T, and the reader is referred to §§ 2 and 3 of that paper for details. When the waves are travelling against the wind ($c < 0$), the air velocities are positive everywhere in the frame of reference moving with the waves. Thus the relaxation method described in the appendix of Taylor, Gent & Keen (1976) can be used to solve the differential equations. This method was used in preference to artificial compressibility for $c < 0$ as the computations converged more rapidly.

3. Variable roughness length

Results will be presented later in this paper where the roughness length is allowed to vary with position along the wave. This is to try to model the effect of shorter gravity and capillary waves, which were shown to be steepest just forward of the crest by Longuet-Higgins (1969*a*). Keller & Wright (1975) have recently made observations of this effective change in roughness and found the maximum roughness to occur between 30° and 60° forward of the crest depending upon u_0 and ak; see their figure 6. Thus there is some support for taking z_0 to be of the form

$$z_0 = \bar{z}_0[1 - \gamma \cos(k\xi \mp \tfrac{1}{4}\pi)] \quad \text{for} \quad c \gtrless 0. \tag{3.1}$$

γ is given the value 0·5 when $ak = 0{\cdot}01$, increasing to 0·75 when $ak = 0{\cdot}157$. The variation of z_0 is introduced into the program through a wall-layer approximation described in § 5 of G & T. There is one small, but interesting, difference however. Taking the square root of equation (5.4) of G & T gives

$$\lambda \bar{E} = |\phi\eta + \tau_0| = |\tau|, \tag{3.2}$$

where $\tau_0(\xi)$ is the surface shear stress and $\phi(\xi) = \overline{p_\xi^* \eta}$. Thus, in the wall layer, the turbulent energy is proportional to the modulus of the shear stress, which is often assumed as a turbulent closure, e.g. see Townsend (1972). In some computations presented later in this paper, the surface stress is negative over some regions of the wave surface. Thus $\tau_0 \gg \phi\eta$ does not hold everywhere and $\bar{U}$ in the wall layer must be calculated from

$$(J^{\frac{1}{2}}\bar{U})_\eta = |\phi\eta + \tau_0| \operatorname{sgn}(\phi\eta + \tau_0)/\kappa(J^{-\frac{1}{2}}\eta + z_0) \tag{3.3}$$

in these regions, and not from equation (5.6) of G & T. It is shown in a note on separation over short wind waves by Gent & Taylor (1977) that separation over water waves

ak	Phase of pressure maximum from trough in x		$\frac{p_{max}-p_{min}}{\rho u_0^2}$	Phase of stress maximum from crest in x		$\frac{\tau_{max}-\tau_{min}}{\rho u_0^2}$	Pressure contribution p_x	Fractional rate $\zeta = 2p_x/(ak)^2$ of energy supply in units of $\frac{\rho_a}{\rho_w}\left(\frac{u_0}{c}\right)^2$
0·01	0·009	3·3°	22·1 (2210ak)	−0·056	−20·2°	0·19 (19ak)	0·0022	−44
0·05	0·008	3°	106·9 (2138ak)	−0·051	−18·3°	0·93 (18·6ak)	0·054	−43·4
0·1	0·01	3·7°	193 (1930ak)	−0·044	−15·9°	1·65 (16·5ak)	0·201	−41·3
0·157	0·014	5·1°	246 (1564ak)	−0·037	−13·4°	1·97 (12·5ak)	0·451	−36·6
0·226	0·021	7·5°	248 (1107ak)	−0·034	−12·1°	2 (8·9ak)	0·741	−29·4
0·314	0·035	12·6°	212 (675ak)	−0·024	−8·5°	2·01 (6·4ak)	1·066	−21·6

TABLE 1. $R=9$, $c=-14$ u_0, z_0 constant.

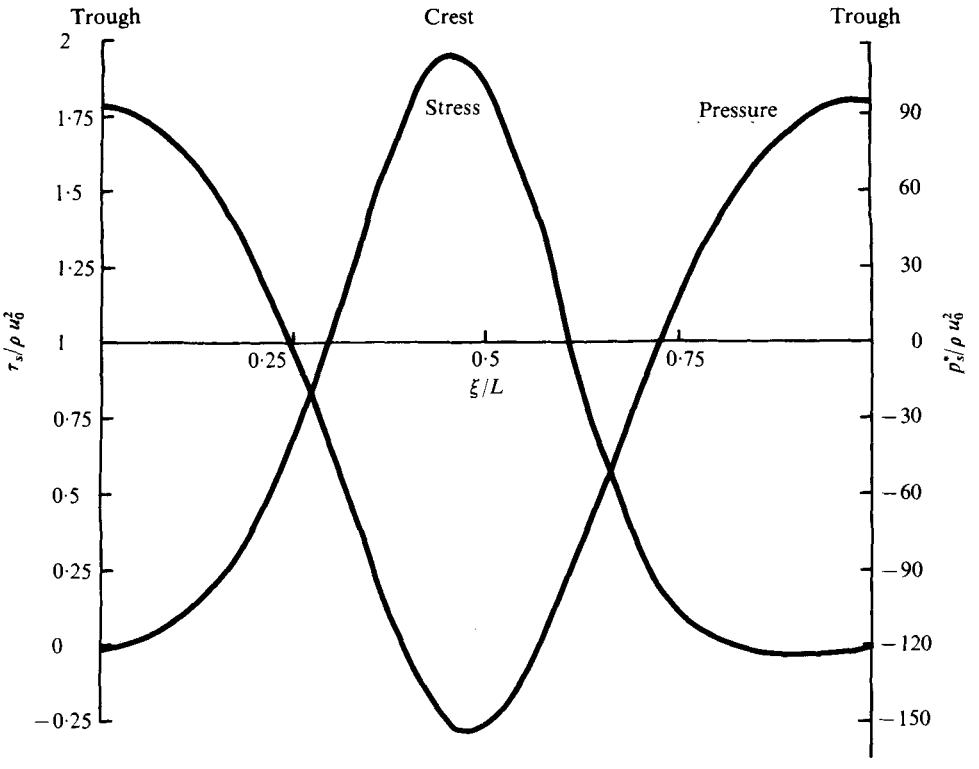

FIGURE 1. Surface pressure and shear stress for $R = 9$, $c = -14u_0$, $ak = 0{\cdot}157$ and z_0 constant.

does not occur at points where the shear stress is zero, and that regions of negative surface shear stress do not qualitatively alter the streamline pattern in the air flow above the waves.

4. Nonlinearity

In G & T, the approach was to keep the wavelength, and hence the phase speed, of the wave fixed, and to alter U_5/c by assuming different values for the friction velocity u_0, and hence U_5. In this paper the approach will be different. We assume fixed values of 0·005 cm and 15 cm/s respectively for the roughness length z_0 and u_0. This gives $U_5 = 28{\cdot}78u_0$ from the logarithmic formula

$$\frac{U_5}{u_0} = \frac{1}{\kappa} \ln \frac{z_5 + z_0}{z_0} \tag{4.1}$$

for flow over a plane surface with $\kappa = 0{\cdot}4$. Thus the wind at 5 m is fixed at a value of 4·32 m/s. U_5/c is now varied by altering the wavelength of the waves. A value is first chosen for the quantity R defined by (cf. Townsend 1972)

$$R \equiv -\ln kz_0. \tag{4.2}$$

This determines the wavenumber k, the phase speed, assumed to be $c = (g/k)^{\frac{1}{2}}$, and hence the value of c/u_0, which, for convenience, is rounded to the nearest integer.

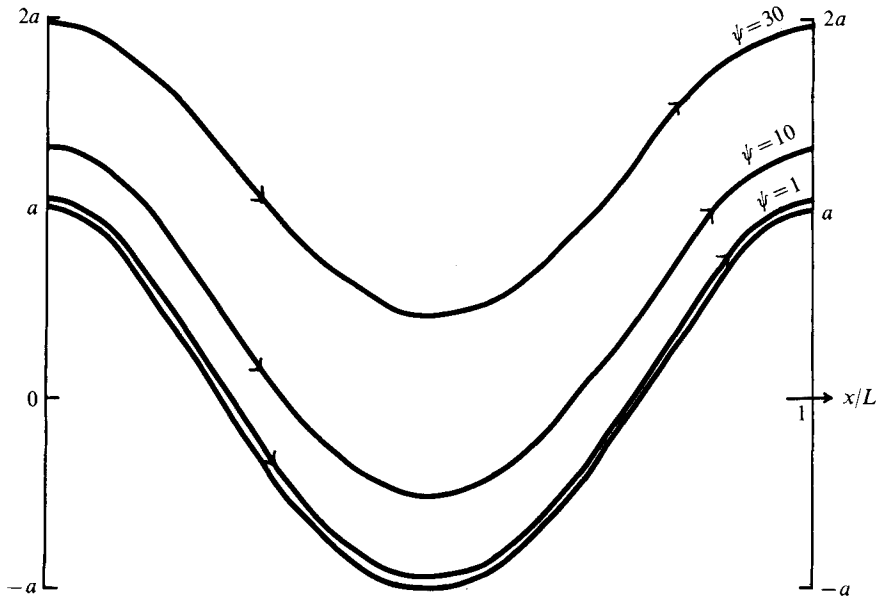

FIGURE 2. Streamlines for same run as figure 1. Vertical scale × 10.

To show the nonlinear effects two series of computations were made at fixed wavelengths with z_0 constant and with the wave amplitude increasing up to $ak = 0{\cdot}314$, or $a = \frac{1}{20}L$. The series were selected as typical of the two regions of parameter space where the energy transfer is from the waves to the wind. The first (table 1) has the waves travelling against the wind with $R = 9$ and corresponds to $L = 2{\cdot}55\,\text{m}$, $c = -1{\cdot}99\,\text{m/s}$ and $U_5/c = -2{\cdot}17$. Linear theories predict constant phases and magnitudes, expressed as multiples of ak, for the pressure and stress. Table 1 shows how these quantities vary as ak increases. The variations in the phases are relatively small, but both the decrease in the magnitudes and the asymmetry of the pressure field are significant as ak increases. The fractional rate ζ of energy transfer per radian advance in phase is given by

$$\zeta = \langle -c(\overline{p} + \overline{w'^2})\, dz_b/dx \rangle, \tag{4.3}$$

where the angle brackets denote an average over the wave form and z_b is the wave surface shape given by equations (2.1) and (2.3) in G & T. Table 1 shows that $|\zeta|$ decreases markedly as ak increases. These results confirm the conclusion in G & T that the nonlinearity of the flow becomes important when $ak > 0{\cdot}05$. Figure 1 shows the surface pressure and stress for $R = 9$, $c = -14u_0$ and $ak = 0{\cdot}157$. There are three points to note. First, the $+x$ direction is always the wind direction in a stationary frame. Thus the waves are propagating in the $-x$ direction, and so a positive phase shift of the pressure maximum, from its equilibrium position over the trough, corresponds to energy transfer from the waves to the wind due to form drag. Second, at this value of ak and as a consequence of nonlinearity, the distributions are not of the pure sinusoidal form predicted by linear theory. Third, the stress is negative in a small region around the trough, but this does not imply separation (see Gent & Taylor 1977) and leaves the streamline pattern in the frame moving with the waves quali-

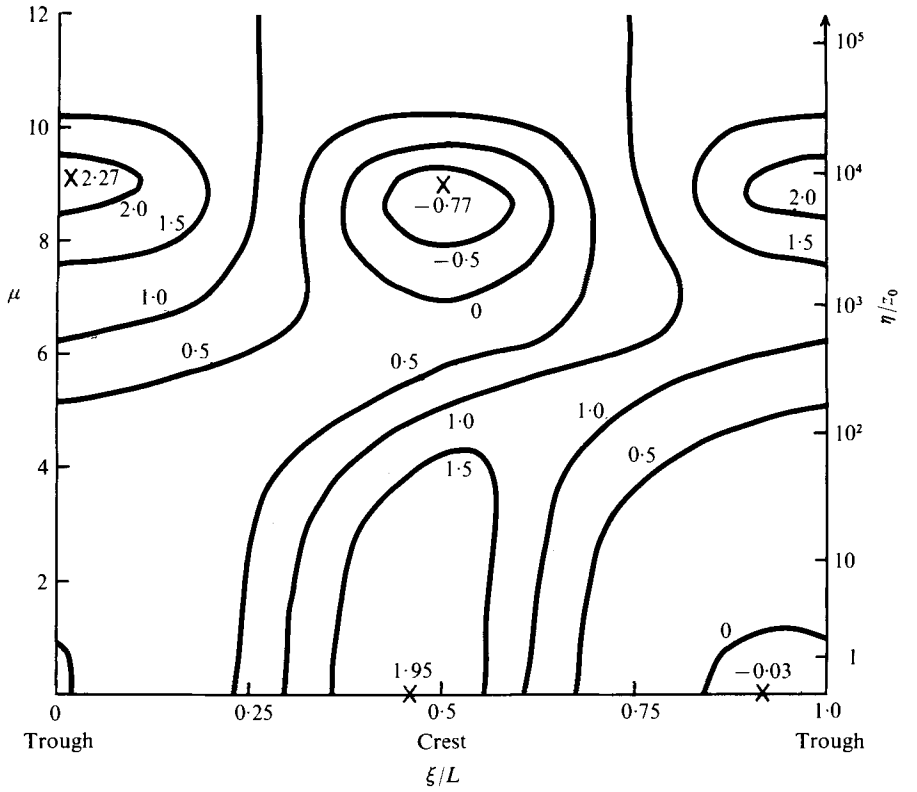

FIGURE 3. Shear-stress contours for same run as figure 1. Logarithmic vertical scale.

tatively unaltered. The pattern is shown in figure 2; the streamlines were calculated from

$$\int_{z_b}^{z} (U_c - c)\, dz, \tag{4.4}$$

where U_c is the Cartesian velocity in the x direction, and are plotted *vs.* x and z, with the vertical scale multiplied by a factor of ten. When the waves are against the wind there is no critical layer and so, incidentally, the Miles shear-flow mechanism cannot work in reverse. The streamline pattern has no region of closed streamlines and just follows the surface in the $+x$ direction. Figure 3 shows shear-stress contours for the same run in order to emphasize the prediction of elevated stress extrema. In this case, they are the absolute extrema, the elevated range being $\approx 3\rho_a u_0^2$ compared with the surface range of $\approx 2\rho_a u_0^2$. The elevated extrema occur at a height of about $0{\cdot}1L$ and a little downwind of the surface extrema, and are almost π out of phase with them. This is a general feature of all the results but may depend upon the closure hypotheses. The vertical scale in figure 3 is logarithmic and the surface features reach to a height of only about $0{\cdot}006L$.

The second series of computations is shown in table 2, and has $R = 11$ with $L = 18{\cdot}8$ m, $c = 5{\cdot}42$ m/s and $U_5/c = 0{\cdot}8$. Here the waves are travelling in the same direction as, but faster than, the wind, and the energy transfer is from the waves to

ak	Phase of pressure maximum from trough in x		$\frac{p_{max}-p_{min}}{\rho u_0^2}$	Phase of stress maximum from crest in x		$\frac{\tau_{max}-\tau_{min}}{\rho u_0^2}$	Pressure contribution p_x	Fractional rate $\zeta = 2p_x/(ak)^2$ of energy supply in units of $\frac{\rho_a}{\rho_w}\left(\frac{u_0}{c}\right)^2$
0·01	−0·013	−4·8°	2·46 (246ak)	−0·459	−165·2°	0·097 (9·7ak)	−0·0005	−10
0·05	−0·015	−5·5°	12·35 (247ak)	−0·456	−164·3°	0·485 (9·7ak)	−0·0123	−9·84
0·1	−0·018	−6·6°	25 (250ak)	−0·453	−163°	0·96 (9·6ak)	−0·05	−10
0·157	−0·022	−8·1°	40·3 (256ak)	−0·448	−161·4°	1·5 (9·5ak)	−0·127	−10·3
0·226	−0·029	−10·5°	59·3 (264ak)	−0·441	−158·6°	2·08 (9·3ak)	−0·27	−10·74
0·314	−0·042	−15·2°	85·5 (272ak)	−0·425	−153°	2·78 (8·8ak)	−0·56	−11·35

TABLE 2. $R = 11$, $c = 36u_0$, z_0 constant.

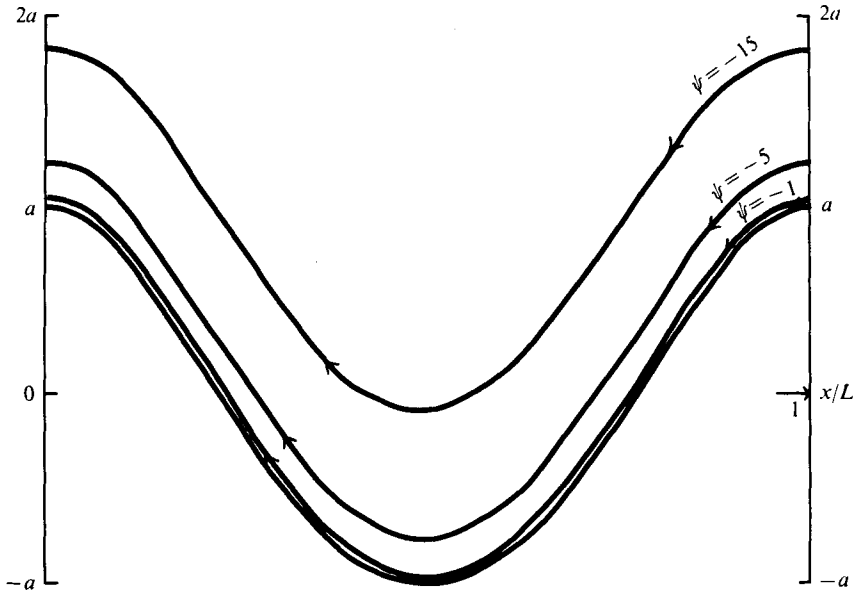

FIGURE 4. Streamlines for $R = 11$, $c = 36u_0$, $ak = 0{\cdot}157$ and z_0 constant. Vertical scale × 10.

the wind. Table 2 again shows only small variations in the phases in contrast to the cases given in G & T. It is interesting that in table 2 the magnitudes of the pressure and $|\zeta|$ do increase slightly as ak increases. For $R = 11$ and $c = 36u_0$, the critical layer is high: at about $190a$ according to (4.1) for $ak = 0{\cdot}157$. It should be noted that the model predicts reduced winds at 5 m compared with (4.1) when u_0 is held fixed, and this slight reduction increases with increasing ak. When calculating U_5/c, however, (4.1) has been used and this variation ignored. This effect would tend to increase the height of the critical layer, which is well above the top of the model, which is at about $1{\cdot}2L$ or $48a$. The streamline pattern in the frame moving with the waves is shown in figure 4 and, like that in figure 2, is relatively unexciting, since it is below the closed-streamline region, and again just follows the surface but this time in the $-x$ direction.

5. Energy transfer from wind to waves

Tables 3 and 4 give series of results when the waves are travelling in the same direction as the wind for z_0 constant and varying respectively. The range of R used was limited at the upper end by the amount of computer time used for long waves and at the lower end by a reluctance to apply the model's closure hypotheses to flow over very short waves. When $R = 6$, the wavelength is 12·67 cm and the critical layer is at $2{\cdot}32z_0$, which is well inside the viscous sublayer, whose depth is $\approx 5\nu/u_0$. The model neglects details of the viscous sublayer, where the velocity profile is linear, however, and assumes the logarithmic form right down to the surface.

In figure 5 the phases of the pressure maximum (always calculated relative to the wave trough) from table 3 (z_0 constant) are plotted against c/u_0 together with the results from table 3 in G & T, in order to compare the results from the two different approaches. Note that the limits shown are for $ak = 0{\cdot}01$ and $0{\cdot}157$ and that in most cases results

R	ak	c/u_0	Phase of pressure maximum from trough in x		$\frac{p_{max}-p_{min}}{\rho u_0^2}$	Phase of stress maximum from crest in x		$\frac{\tau_{max}-\tau_{min}}{\rho u_0^2}$	Pressure contribution p_x	Fractional rate $\zeta = 2p_x/(ak)^2$ of energy supply in units of $\frac{\rho_a}{\rho_w}\left(\frac{u_0}{c}\right)^2$
10·75	0·01	32	−0·017	−6·3°	1·24 (124ak)	−0·456	−164.·1°	0·083 (8·3ak)	−0·0003	−6
10·75	0·157	32	−0·03	−10·6°	21·26 (135·4ak)	−0·445	−160·2°	1·28 (8·2ak)	−0·084	−6·84
10·5	0·01	28	−0·023	−8·2°	0·449 (44·9ak)	−0·452	−162·6°	0·069 (6·9ak)	−0·0002	−4
10·5	0·157	28	−0·043	−15·4°	8·54 (54·4ak)	−0·441	−158·7°	1·072 (6·8ak)	−0·044	−3·59
10·25	0·01	25	0·02	7°	0·178 (17·8ak)	−0·45	−161·8°	0·061 (6.1ak)	0·0001	2
10·25	0·157	25	−0·023	−8·4°	3·64 (23·1ak)	−0·436	−156·9°	0·939 (6ak)	−0·006	−0·47
10	0·01	22	0·216	77·9°	0·257 (25·7ak)	−0·426	−153·5°	0·057 (5·7ak)	0·0006	12
10	0·157	22	0·149	53·4°	2·56 (16·3ak)	−0·428	−154°	0·83 (5·3ak)	0·055	4·46
9·5	0·01	17	0·202	72·7°	0·383 (38·3ak)	−0·351	−126·5°	0·043 (4·3ak)	0·001	20
9·5	0·157	17	0·301	108·5°	4·2 (26·7ak)	−0·372	−133·9°	0·646 (4·1ak)	0·17	13·8
9	0·01	14	0·136	49°	0·492 (49·2ak)	−0·281	−101·1°	0·038 (3·8ak)	0·0009	18
9	0·157	14	0·228	82·1°	5·41 (34·5ak)	−0·312	−112·4°	0·53 (3·4ak)	0·205	16·6
8	0·01	8	0·045	16·2°	1·35 (135ak)	−0·144	−51·9°	0·043 (4·3ak)	0·0009	18
8	0·157	8	0·098	35°	14·7 (93·6ak)	−0·099	−35·8°	0·59 (3·8ak)	0·19	15·4
7	0·01	5	0·039	14·1°	1·54 (154ak)	−0·114	−41·1°	0·059 (5·9ak)	0·0009	18
7	0·157	5	0·079	28·5°	18·6 (118ak)	−0·079	−28·5°	0·778 (5ak)	0·196	15·9
6	0·01	3	0·041	14·8°	1·44 (144ak)	−0·103	−37°	0·072 (7·2ak)	0·0009	18
6	0·157	3	0·078	27·9°	18·1 (115ak)	−0·071	−25·7°	0·954 (6·1ak)	0·193	15·6

TABLE 3. z_0 constant.

R	ak	γ	c/u_0	Phase of pressure maximum from trough in x		$\frac{p_{max}-p_{min}}{\rho u_0^2}$	Phase of stress maximum from crest in x		$\frac{\tau_{max}-\tau_{min}}{\rho u_0^2}$	Pressure contribution p_x	Fractional rate $\zeta = 2p_x/(ak)^2$ of energy supply in units of $\frac{\rho_a}{\rho_w}\left(\frac{u_0}{c}\right)^2$
11	0·01	0·5	36	−0·009	−3·1°	2·35 (235ak)	0·239	86·2°	0·225 (22·5ak)	−0·0003	−6
11	0·05	0·6	36	−0·014	−5·1°	11·8 (236ak)	0·393	141·4°	0·363 (7·3ak)	−0·011	−8·7
11	0·157	0·75	36	−0·023	−8·2°	35·9 (228ak)	0·44	158·3°	1·27 (8·5ak)	−0·114	−9·2
10·75	0·01	0·5	32	−0·01	−3·5°	1·16 (116ak)	0·225	81°	0·235 (23·5ak)	−0·0002	−4
10·75	0·157	0·75	32	−0·03	−10·9°	18·4 (117ak)	0·432	155·7°	1·08 (6·9ak)	−0·073	−5·9
10·5	0·01	0·5	28	−0·012	−4·5°	0·403 (40·3ak)	0·213	76·6°	0·246 (24·6ak)	−0·0001	−2
10·5	0·157	0·75	28	−0·044	−16°	6·94 (44·2ak)	0·424	152·5°	0·89 (5·7ak)	−0·035	−2·8
10·25	0·01	0·5	25	−0·04	−14·5°	0·16 (16ak)	0·206	74·1°	0·255 (25·5ak)	−0·0001	−2
10·25	0·157	0·75	25	−0·004	−1·6°	2·97 (18·9ak)	0·418	150·4°	0·76 (4·9ak)	0·004	0·3
10	0·01	0·5	22	−0·004	−1·4°	0·327 (32·7ak)	0·204	73·4°	0·263 (26·3ak)	0	$-1 < \zeta < 0$
10	0·157	0·75	22	0·173	62·4°	2·7 (17·2ak)	0·416	149·8°	0·64 (4·1ak)	0·072	5·9
9·5	0·01	0·5	17	0·102	36·8°	1·03 (103ak)	0·192	69·3°	0·242 (24·2ak)	0·0016	32
9·5	0·157	0·75	17	0·261	94°	4·85 (30·9ak)	0·42	151·3°	0·4 (2·5ak)	0·183	14·8
9	0·01	0·5	14	0·128	46°	1·38 (138ak)	0·159	57·4°	0·236 (23·6ak)	0·0025	50
9	0·157	0·75	14	0·191	68·8°	6·44 (41ak)	0·43	154·6°	0·23 (1·5ak)	0·228	18·5
8	0·01	0·5	8	0·116	41·7°	1·95 (195ak)	0·097	34·8°	0·308 (30·8ak)	0·0031	62
8	0·157	0·75	8	0·109	39·2°	15·35 (97·7ak)	−0·044	−15·8°	0·57 (3·6ak)	0·231	18·7
7	0·01	0·5	5	0·118	42·5°	2·13 (213ak)	0·083	30°	0·387 (38·7ak)	0·0035	70
7	0·157	0·75	5	0·095	34·1°	18·76 (119ak)	−0·033	−11·7°	0·86 (5·5ak)	0·244	19·8
6	0·01	0·5	3	0·132	47·5°	2·12 (212ak)	0·079	28·3°	0·467 (46·7ak)	0·0037	74
6	0·157	0·75	3	0·098	35·3°	18 (114ak)	−0·025	−9°	1·14 (7·2ak)	0·245	19·8

TABLE 4. z_0 varying: $z_0 = \bar{z}_0\,[1-\gamma\cos(k\xi-\frac{1}{4}\pi)]$.

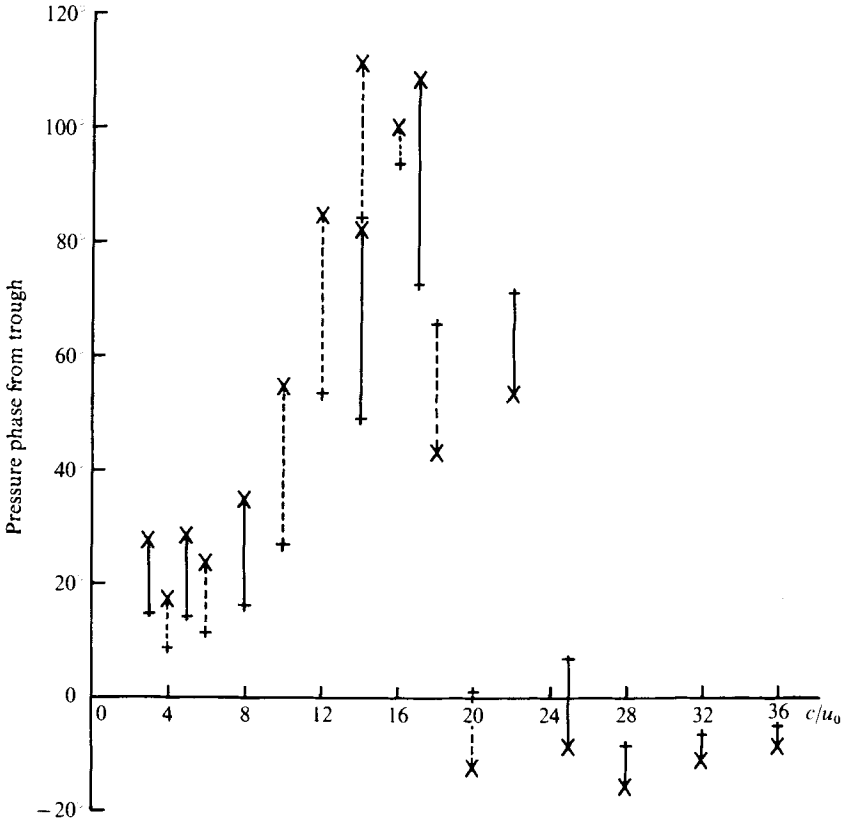

FIGURE 5. Phase difference of pressure maximum measured from wave trough against c/u_0 for z_0 constant. +, $ak = 0{\cdot}01$; ×, $ak = 0{\cdot}157$; ——, table 3; – – –, table 3 of G & T.

for intermediate values of ak would lie on the line joining these two values; also note that the $R = 8$, $c = 8u_0$ results are common to both series. Figure 5 shows that the overall shape of the two sets of results is very similar, as is the maximum predicted phase shift of about 110°. However, for $c > 8u_0$ the results when u_0 is fixed and c varies are shifted to somewhat higher c/u_0 than the curve for fixed c and variable u_0. The limits $c/u_0 \to 0$ are different. The phase is 10°–15° and decreasing in the limit of no wind over a fixed wave, whereas it is about 15°–25° and almost constant in the limit of short waves with a given wind speed. This difference is due to the different values of L/z_0 in the two cases. More interesting, however, is the value of c/u_0 where the model predicts zero pressure phase. This is $c/u_0 \approx 20$ for a fixed wavelength but $c/u_0 \approx 25$ for a fixed wind. This value is the important factor in determining the value of U_5/c where the pressure phase is zero, although z_0 also affects the value through the ratio U_5/u_0. The results show that the value of U_5/c where the pressure phase is zero will decrease with increasing wavelength, and that variations in this 'critical' value of U_5/c are to be expected. There is considerable scatter in the observed values (see figure 6) and more will be said on this subject in § 7.

Figure 6 is a plot against U_5/c of the phase of the pressure maximum for computations with z_0 varying from table 4. As in G & T, for $ak = 0{\cdot}01$ and $\gamma = 0{\cdot}5$ this reduces the maximum phase to about 45°, but for $ak = 0{\cdot}157$ and $\gamma = 0{\cdot}75$ the variable surface

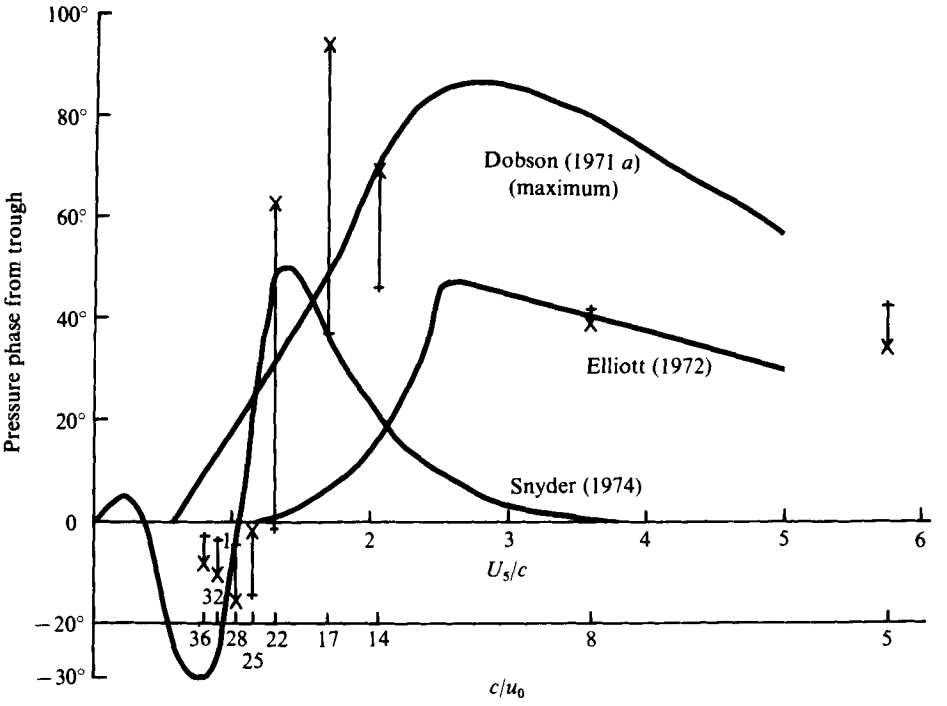

FIGURE 6. Phase difference of pressure maximum measured from wave trough against U_5/c for z_0 varying. +, $ak = 0{\cdot}01$, $\gamma = 0{\cdot}5$; ×, $ak = 0{\cdot}157$, $\gamma = 0{\cdot}75$. From table 4.

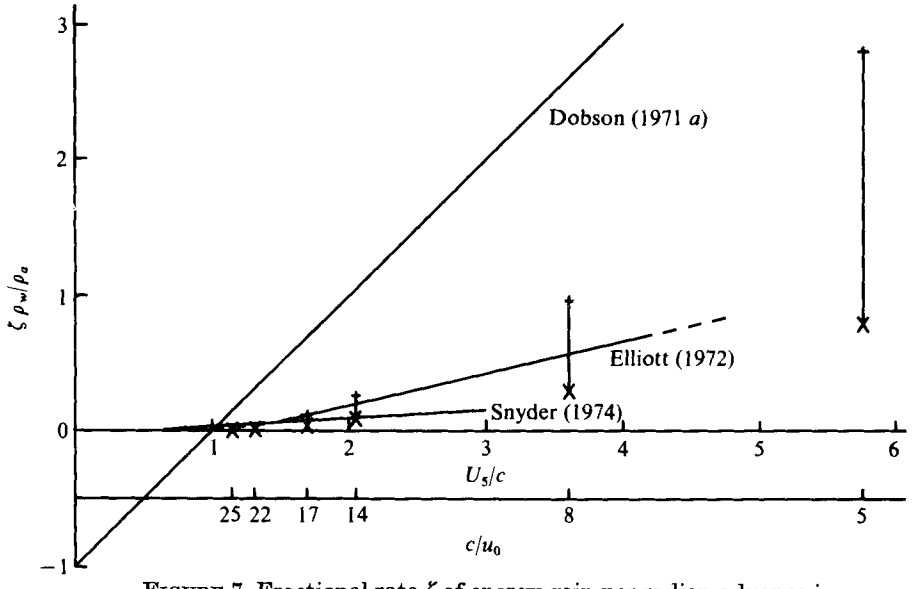

FIGURE 7. Fractional rate ζ of energy gain per radian advance in phase against U_5/c. Same notation as in figure 6.

roughness has little effect, and the values are close to those for z_0 constant. Also plotted in figure 6 are the observations of Dobson (1971*a*), Elliott (1972) and Snyder (1974). Although there is wide scatter in the observations, it may be said, in general, that the z_0-varying results for very small amplitude are more in line with the observations, especially those of Elliott. The model always predicts very high gradients of pressure phase for values of U_5/c just larger than the value where the phase is zero, and so a small change in U_5/c makes a large difference to the pressure phase. Thus gustiness in the wind, causing changes of say 10–20 % in U_5/c, is predicted to cause large changes in the pressure phase, and this may well be one reason for the large scatter in the observations at sea. Another difficulty arises from the Fourier analysis of observations, since this relies on linearity and assumes no phase variation with wave height. Figure 7 shows the rate ζ of energy input per radian advance in phase plotted against U_5/c for z_0 varying (see table 4). The higher values are for $ak = 0{\cdot}01$ and $\gamma = 0{\cdot}5$ while the lower values are for $ak = 0{\cdot}157$ and $\gamma = 0{\cdot}75$, which are similar to the constant-z_0 values. Also plotted are the observations of Dobson, Elliott and Snyder. Detailed comparisons are made in G & T, but it should be noted that the $ak = 0{\cdot}01$ values are between two and three times the predictions from linear theories, and again our results compare best with Elliott's observations. Preliminary results from the most recent observations in the Bight of Abaco by Dobson, Elliott, Long & Snyder (private communication) suggest values of ζ similar to those of Elliott (1972).

6. Energy transfer from waves to wind

Phillips (1966, p. 148) says that 'The processes involved in the attenuation of the longer gravity waves have been almost as elusive as those of generation.' Nonlinear wave–wave interaction must play an important role in the attenuation of long gravity waves and swell, and will probably be the dominant factor when the waves propagate with the wind. Energy transfer to the wind may be an important factor, however, when the waves are against the wind. Both cases will be considered.

Some results for cases when the waves are travelling faster than the wind are given in tables 3 and 4. The pressure phases (figures 5 and 6) have minima of approximately $-15°$ occurring at $c \approx 28u_0$, or $U_5/c \approx 1$, and then the phases slowly tend towards zero as U_5/c decreases and c/u_0 increases. The minimum value of U_5/c for which we have results is 0·8, but we should expect the pressure phases to continue to be negative and to tend to zero as $U_5/c \to 0$. These phases compare best with Snyder's (1974) observations (see figure 6). The general pattern of our predictions compares well with his observations (his figure 18), whose minimum is at $U_5/c \approx 0{\cdot}8$, but the observational minimum is somewhat lower, at about $-30°$, and the phase does become positive again for U_5/c closer to zero. However, the agreement is encouraging. Dobson (1971*a*) still has positive phases for c/u_0 up to 40, while Elliott (1972) has a few observations of negative phases for $1 < U_5/c < 2$ but observed a greater number of positive phases in the same range.

From tables 3 and 4 it is clear that the magnitude of the pressure field has a minimum at $c \approx 25u_0$, but then increases rapidly as c/u_0 increases. When the waves propagate faster than the wind, however, the pressure phase is small, and this also keeps the energy input rate ζ calculated from (4.3) small. Expressed as a multiple of $(\rho_a/\rho_w)(u_0/c)^2$, it lies in the range $-10 < \zeta < 0$, and it should be noted that the predictions of the

R	ak	c/u_0	Phase of pressure maximum from trough in x		$\frac{p_{max}-p_{min}}{\rho u_0^2}$	Phase of stress maximum from crest in x		$\frac{\tau_{max}-\tau_{min}}{\rho u_0^2}$	Pressure contribution p_x	Fractional rate $\zeta = 2p_x/(ak)^2$ of energy supply in units of $\frac{\rho_a}{\rho_w}\left(\frac{u_0}{c}\right)^2$
6	0·01	−3	0·025	9·1°	4·4 (440ak)	−0·074	−26·7°	0·14 (14ak)	0·0013	−26
6	0·157	−3	0·042	15·3°	55·3 (269ak)	−0·051	−18·5°	1·79 (11·4ak)	0·28	−22·7
7	0·01	−5	0·013	4·5°	7·5 (750ak)	−0·074	−26·7°	0·15 (15ak)	0·0015	−30
7	0·157	−5	0·029	10·4°	90·3 (575ak)	−0·047	−16·9°	1·84 (11·7ak)	0·319	−25·9
8	0·01	−8	0·01	3·6°	12·2 (1220ak)	−0·063	−22·8°	0·163 (16·3ak)	0·0018	−36
8	0·157	−8	0·021	7·7°	144 (916ak)	−0·042	−15·3°	1·88 (12ak)	0·368	−29·8
10	0·01	−22	0·003	1·1°	38·2 (3820ak)	−0·052	−18·6°	0·225 (22·5ak)	0·0027	−54
10	0·157	−22	0·01	3·7°	398 (2536ak)	−0·032	−11·7°	2·02 (12·9ak)	0·565	−45·8
11	0·01	−36	0·003	1·1°	72·5 (7250ak)	−0·043	−15·6°	0·285 (28·5ak)	0·0035	−70
11	0·157	−36	0·008	3°	675 (4294ak)	−0·028	−10·1°	2·2 (14ak)	0·781	−63·3

TABLE 5. z_0 constant.

R	ak	γ	c/u_0	Phase of pressure maximum from trough in x		$\frac{p_{max}-p_{min}}{\rho u_0^2}$	Phase of stress maximum from crest in x		$\frac{\tau_{max}-\tau_{min}}{\rho u_0^2}$	Pressure contribution p_x	Fractional rate $\zeta = 2p_x/(ak)^2$ of energy supply in units of $\frac{\rho_a}{\rho_w}\left(\frac{u_0}{c}\right)^2$
6	0·01	0·5	−3	0·017	6·1°	5·6 (560ak)	−0·137	−49·4°	0·638 (63·8ak)	0·0017	−34
6	0·157	0·75	−3	0·049	17·6°	52·0 (331ak)	−0·062	−22·4°	2·07 (13·2ak)	0·278	−22·5
7	0·01	0·5	−5	0·013	4·5°	8·5 (850ak)	−0·134	−48·2°	0·58 (58ak)	0·002	−40
7	0·157	0·75	−5	0·033	11·8°	86·2 (549ak)	−0·057	−20·6°	2·09 (13·3ak)	0·32	−26
8	0·01	0·5	−8	0·014	5·2°	13·1 (1310ak)	−0·13	−46·7°	0·534 (53·4ak)	0·0023	−46
8	0·157	0·75	−8	0·023	8·2°	141·7 (903ak)	−0·052	−18·8°	2·15 (13·7ak)	0·377	−30·6
9	0·01	0·5	−14	0·005	1·8°	22·7 (2270ak)	−0·12	−43°	0·513 (51·3ak)	0·0027	−54
9	0·05	0·6	−14	0·009	3·2°	108·2 (2164ak)	−0·075	−26·9°	1·256 (25·1ak)	0·0575	−46
9	0·157	0·75	−14	0·015	5·3°	244·4 (1557ak)	−0·046	−16·5°	2·22 (14·1ak)	0·459	−37·2
10	0·01	0·5	−22	0·006	2°	38·8 (3880ak)	−0·109	−39·2°	0·503 (50·3ak)	0·0032	−64
10	0·157	0·75	−22	0·011	3·9°	396 (2523ak)	−0·04	−14·3°	2·22 (14·1ak)	0·569	−46·2
11	0·01	0·5	−36	0·003	1·1°	73·1 (7310ak)	−0·094	−33·9°	0·526 (52·6ak)	0·004	−80
11	0·157	0·75	−36	0·008	3°	680 (4332ak)	−0·034	−12·3°	2·36 (15ak)	0·78	−63·3

TABLE 6. z_0 varying: $z_0 = \bar{z}_0\,[1-\gamma\cos(k\xi+\frac{1}{4}\pi)]$.

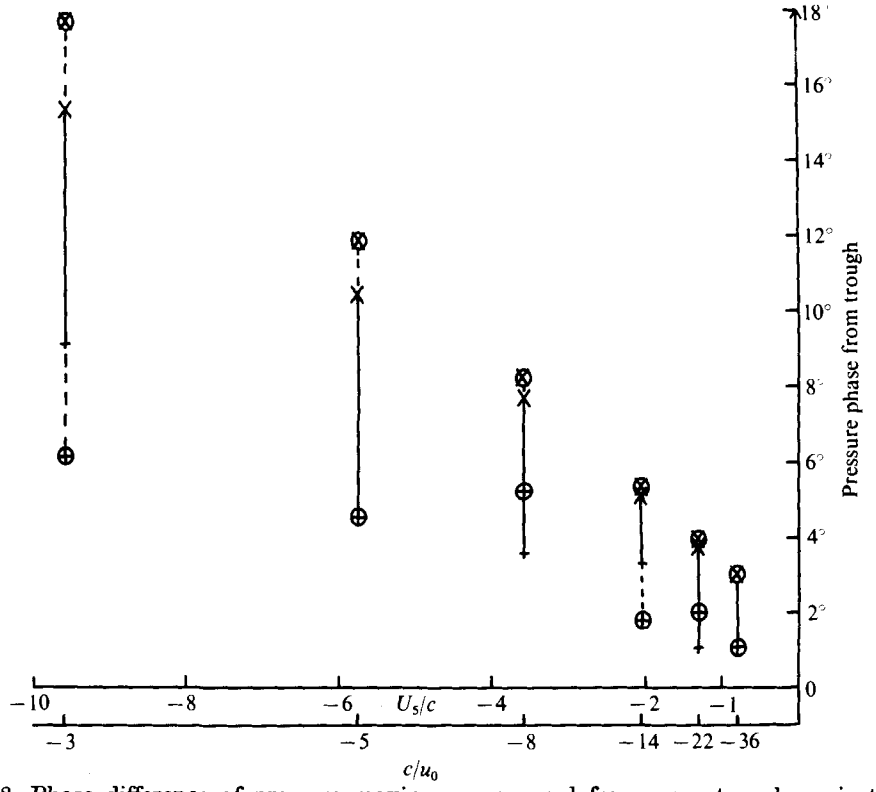

FIGURE 8. Phase difference of pressure maximum measured from wave trough against U_5/c. +, $ak = 0{\cdot}01$; ×, $ak = 0{\cdot}157$; ——, z_0 constant; ⊕, $ak = 0{\cdot}01$, $\gamma = 0{\cdot}5$; ⊗, $ak = 0{\cdot}157$, $\gamma = 0{\cdot}75$; – – –, z_0 varying.

pressure phase and ζ for z_0 constant and varying are very similar in this region of parameter space. If the values of $|\zeta|(\rho_w/\rho_a)\,(c/u_0)^2$ in tables 3 and 4 were constant as U_5/c decreased, then, for constant u_0, $|\zeta|$ would decrease as c^{-2}, i.e. in inverse proportion to the wavelength. Thus we predict that the attenuation rate due to form drag for waves travelling faster than the wind decreases almost as fast as L^{-1}.

Several runs have been made when the waves are travelling against the wind ($c < 0$) and the results for constant z_0 are shown in table 5. The shorter gravity and capillary waves will probably still be on the forward slope of the longer waves (in the direction of travel), so the roughness maximum is $\frac{1}{4}\pi$ backwards from the crest in terms of $k\xi$, since the positive direction is that of the wind. Thus the variable-roughness results in table 6 have

$$z_0 = \bar{z}_0[1 - \gamma\cos(k\xi + \tfrac{1}{4}\pi)]. \tag{6.1}$$

The pressure phases from the two tables are plotted against U_5/c in figure 8, which shows them to be very similar. All the phases are relatively small, less than 18°, and decrease monotonically as $|U_5/c|$ decreases. We should expect the phases to continue to tend monotonically towards zero as $U_5/c \to 0$ and not to change sign, so that waves of all wavelengths are attenuated by the action of pressure forces. There are very few observations for comparison. Dobson (1971*b*) observed a group of 3–4 s sea waves in a light adverse wind of 2·2 m/s. Thus $U_5/c \approx -0{\cdot}5$ and the observed phase was

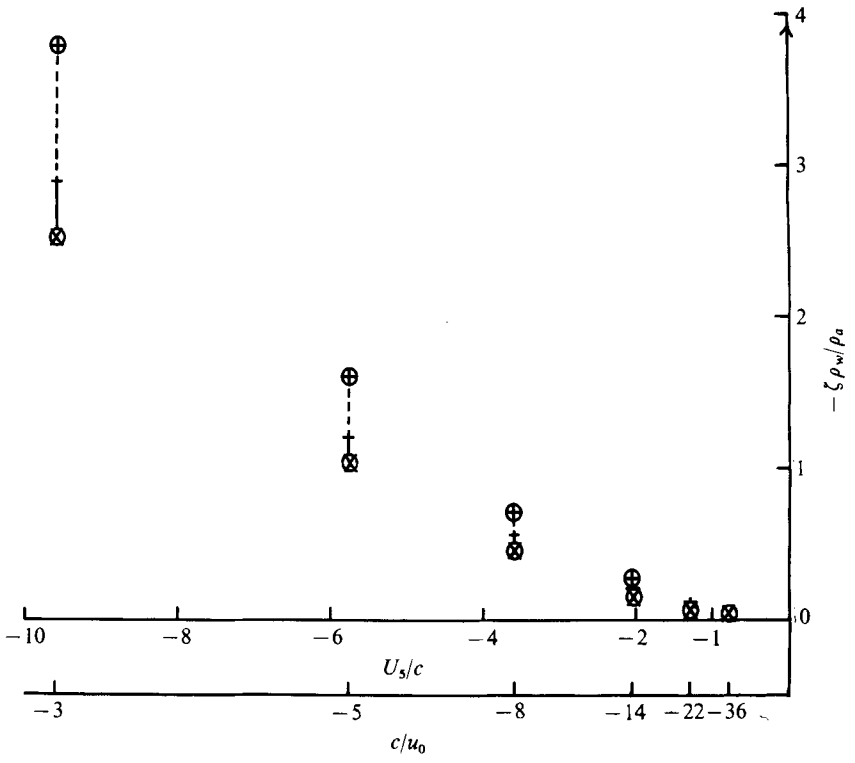

FIGURE 9. Fractional rate $-\zeta$ of energy loss per radian advance in phase against U_5/c. Same notation as in figure 8.

$15° \pm 5°$. This is somewhat larger than our prediction. Dobson (private communication) has recently analysed some data from the Bight of Abaco where the waves were against a very light wind. The pressure phases are both positive and negative and are between $\pm 5°$. This is less than the error bars for the measurements, so that the only safe conclusion is that the phases are very small, in agreement with our model. The only other observations are those of Snyder (1974), which do not agree at all with our predictions. They show large pressure phases, greater than 90°, for $-1 < U_5/c < 0$ and negative phases for $U_5/c < -2$, indicating energy transfer from wind to waves.

In figure 9, $-\zeta$ is plotted against U_5/c from the values in tables 5 and 6. Although the pressure phases are similar for small amplitudes, the increase in pressure magnitude when z_0 varies results in a slightly higher value of $-\zeta$ compared with that for z_0 constant. As always, the values converge as ak increases. For longer waves with small ak, the values of ζ for z_0 constant and varying converge slowly, and both predict a rapid decrease in $|\zeta|$ as the wavelength increases. The energy transfer rate can be compared with the theoretical prediction in Phillips (1966) and the observation of Dobson (1971*b*). Phillips considered the interaction of the turbulence and the wave-induced Reynolds stress and predicted that $-\zeta$ (his μ, figure 4.19) is about 2×10^{-4} when $c = 8u_0$ and increases linearly with c/u_0 to about 5×10^{-4} when $c = 36u_0$. In contrast we predict that, for z_0 constant, $-\zeta$ is about 6×10^{-4} when $c = 8u_0$ and decreases with c/u_0 to about 6×10^{-5} when $c = 36u_0$. In order to make a comparison with Dobson's value we must extrapolate our results to $R = 12$ and $c = 60u_0$. An estimated value of

$-\zeta$ of $105\rho_a/\rho_w\,(u_0/c)^2$ gives $-\zeta = 3{\cdot}5 \times 10^{-5}$, which is an order of magnitude less than Dobson's value of $3{\cdot}8 \times 10^{-4}$. However, it happens to be the exact empirical value calculated by Sverdrup & Munk (1947) in an early analysis of wave data.

Longuet-Higgins (1969*b*) showed that a varying shear stress is dynamically equivalent to a normal pressure fluctuation lagging $\frac{1}{2}\pi$ behind the stress. The average stress at the surface can be thought of as working to produce a mean current or surface wind-drift current, whereas we have calculated the work done on the waves by the varying stress as proportional to $\langle \tau z_b \rangle$. We have not given the values as the energy transfer due to stress is generally small, less that 20 % of that due to pressure, and is a smaller percentage in the main generation and attenuation regions of parameter space.

Short waves propagating into the wind may well not be attenuated, as predicted above, but rather shorten and steepen, and then be dissipated by breaking. This is probably due to the fact that they are propagating into the surface wind-drift current, which is observed to be about 3 % of U_5. This drift current is a sizable fraction of the phase speed of short waves, and can cause them to break; see Gent & Taylor (1977). They also discuss the sensitivity of the model to changes in the kinematic boundary condition at the air–water interface, equation (3.3) of G & T. When the phase speed is much larger than the drift current, however, waves propagating into the wind will be attenuated, so that the above calculations of the energy transfer rates due to form drag are more appropriate to longer waves and swell.

Observations of swell are reported in a series of papers: Barber & Ursell (1948), Munk *et al.* (1963) and Snodgrass *et al.* (1966). Detailed analysis of the observations showed that swell could be identified that had been generated by severe storms as much as 20 000 km away and 20 days before. In one case the swell was generated in the Indian Ocean and passed between Antarctica and New Zealand on its great-circle route to California, where it was observed. In our model, the fractional rate of energy loss decreases rapidly as the wavelength increases both when the wind is in the direction of and when it is against the swell. Because of the very high pressure magnitudes when $c < 0$ (0·02 mbar for $R = 11$ and $ak = 0{\cdot}01$), we predict that the energy transfer rate is higher when the wind is against the swell. Further extrapolation (highly unjustified) of the results in table 6 suggests a maximum value of $200(\rho_a/\rho_w)\,(u_0/c)^2$ for $-\zeta$ when $ak = 0{\cdot}01$ and $R = 14$, which corresponds to very long swell of wavelength 377·8 m and period 15·56 s and to $c = 162u_0$. Thus $-\zeta \approx 9 \times 10^{-6}$ and the wave amplitude will reduce to $e^{-\pi}$, or 4·32 %, of its original value in just under 20 days, having travelled over 40 000 km, or once round the earth. Thus the model predictions are not inconsistent with these swell observations.

7. At what value of U_5/c does the energy transfer change direction?

In observations of pressure phases at sea during active wave generation there is considerable scatter in the value of U_5/c at which the phase is zero, e.g. see figure 6. The range is about $1 < U_5/c < 2$, and all observations show a rapid increase in phase as U_5/c increases; the waves which are most actively generated having a slightly larger value of U_5/c than that for which the phase is zero. In § 5 we described how the method of varying U_5/c affected the value where the pressure phase was zero. We estimated the position of zero pressure phase from the values in tables 3 of this paper and G & T and the values for $R = 8$, 10 and 12 from table 2 of Townsend (1972), all for constant z_0.

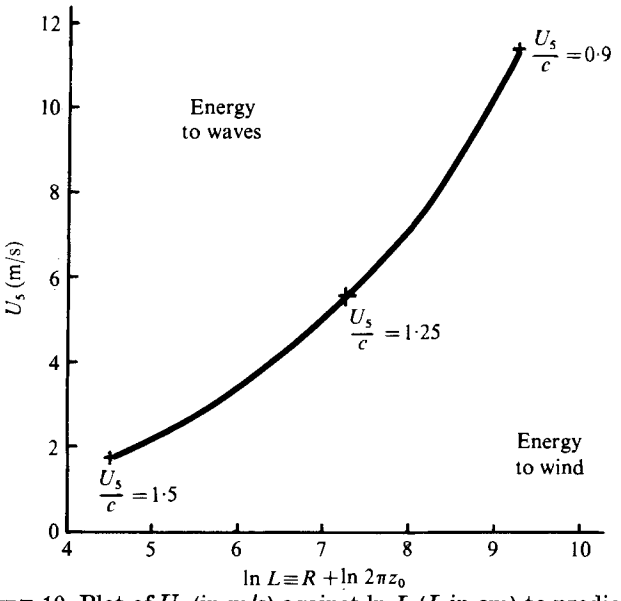

FIGURE 10. Plot of U_5 (in m/s) against $\ln L$ (L in cm) to predict the direction of energy transfer due to form drag. z_0 constant.

We then used three different values of z_0: 0·01, 0·008 and 0·005 cm, which gave us fifteen points to plot, although some were very close together. A smooth curve could be drawn through most of the points and it is shown in figure 10, which is a plot of U_5 in m/s against $\ln L$, where the units of L are cm. Figure 10, then, indicates the direction of energy transfer due to form drag for given wind speeds and wavelengths. It can be only a rough guide, however, as small changes in $\ln L$ when it is large mean considerable changes in the actual wavelength. More interesting, however, is the variation of U_5/c along the line. Its value decreases monotonically from 1·5 when $U_5 \approx 1{\cdot}8$ m/s and $L \approx 0{\cdot}94$ m to 0·9 when $U_5 = 11{\cdot}4$ m/s and $L = 102$ m. Thus we predict that the value of U_5/c where the pressure phase is zero depends upon U_5 or L, and decreases as the wind speed and wavelength increase together.

The effect of allowing the roughness length to vary with position along the wave is to reduce the value of c/u_0 where the pressure phase is zero. The effect of the corresponding increase in the value of U_5/c would be to raise the curve in figure 10 slightly. Movement in the same direction is indicated by considering the working of the variable shear stress on the lower boundary. Here we are considering a region where the pressure transfer is small, so that the transfer due to tangential stress becomes important, and can dominate when ζ is very small. Our calculations indicate that inclusion of the work due to this stress would reduce the value of c/u_0 where the direction of energy transfer changes, again raising the curve in figure 10. This rise due to variable z_0 and the work of the variable surface shear stress could be reversed, however, by wave–wave energy transfer which gives energy to the longer wave components.

The JONSWAP observations by Hasselmann *et al.* (1973) show that the frequency of the peak of the wave spectrum varies with fetch. Their figure 2.6 indicates that a good approximation is that the non-dimensional frequency $f_m U_{10}/g$ at the peak is inversely proportional to the one-third power of the non-dimensional fetch xg/U_{10}^2.

From their observations the non-dimensional peak frequency at the longest fetch, which should correspond most closely to the theoretical results considered here, is 0·17. Using $U_5 = 0{\cdot}94U_{10}$, calculated from (4.1), this gives

$$U_5/c = 0{\cdot}94 \times 2\pi \times f_m U_{10}/g = 1$$

as the minimum value of U_5/c at the peak of the wave spectrum at the longest fetch. This value of U_5/c then increases as the fetch decreases, reaching a value of about 5 for the short-fetch JONSWAP observations.

8. Conclusions

These further results from the numerical model of the steady, nonlinear, turbulent air flow over a train of two-dimensional monochromatic waves confirm the conclusion of G & T that allowing z_0 to vary with position along the wave can increase the energy input rate to small amplitude waves by a factor of between two and three. Here U_5/c is varied by keeping U_5 fixed and varying c, and the graph of pressure phase against U_5/c is shifted to smaller values of U_5/c compared with that in G & T, where c was fixed and U_5 varied. Section 7 shows how the value of U_5/c where the pressure is in exact antiphase with the wave form decreases with increasing U_5 and increasing wavelength.

Further results, presented in § 6, show that the energy transfer due to form drag is predicted to be from the waves to the wind when the waves travel faster than or against the wind. When the wind is against the waves, however, allowing z_0 to vary with position produces little effect upon the energy transfer rates.

In summary, therefore, a variable roughness length only has a dramatic effect in terms of altering the pressure phase and increasing ζ substantially for small ak, when the constant-z_0 pressure phase is large, i.e. in the main generation region. Where we predict wave attenuation, the constant-z_0 pressure phases are small, and here a variable roughness length has only a small effect on the pressure phase and ζ.

Recently three different mechanisms by which short waves can influence the growth or decay of long waves have been investigated. The first is that the wind generates short waves which, if they dissipate preferentially near the long-wave crests owing to the influence of the long-wave field, transfer their momentum to the long waves. From their observations in a wave tank Larson & Wright (1975) suggested that the short waves could support the majority of the wind stress. Their observed growth rates for short waves are supported by the theoretical work of Valenzuela (1976) on short-wave growth due to linear instability of a coupled shear flow. However Garrett & Smith (1976) point out that at most a proportion of the wind stress equal to the long-wave slope can be transferred to the long waves by this mechanism. If the short-wave momentum is not generated solely at the long-wave crests, this proportion will reduce, and they conclude that although this mechanism may be significant for long-wave growth, it cannot account for it entirely.

The second mechanism is the influence of the short waves on the tangential stress and its energy transfer direct to the long waves. From the computations presented in G & T and here, this influence is much smaller than the influence on the energy transfer due to normal stresses, and the values have not been quoted. This is for a monochromatic two-dimensional wave train, however, and Longuet-Higgins (1977)

illustrates that the energy transfer due to tangential stress may be important to relatively steep, dominant waves occurring in groups.

The third mechanism is the influence of the short waves on the energy transfer direct to long waves by normal stresses. This has been the subject primarily addressed in G & T and this work. It should be noted that an additional contribution to the energy transfer has been neglected in these studies. This is

$$\langle -c(\overline{p' \, dz_b'/dx}) \rangle,$$

where p' is the fluctuating pressure and z_b' is the short-wave contribution to z_b. Thus the energy transfer rates may be a little higher than the values presented, which show a dramatic increase for small amplitude long gravity waves.

I should like to thank Dr P. A. Taylor, Dr F. W. Dobson, Dr J. A. Elliott and Professor O. M. Phillips for helpful discussions on this work. All were visited while the author was in receipt of a grant from the Air–Sea Interaction Committee of NATO. The work was partially supported by the Natural Environment Research Council (U.K.) under grant GR3/1932. The paper was written while the author was a summer visitor at Research Establishment Risø, Denmark.

REFERENCES

BARBER, N. F. & URSELL, F. 1948 *Phil. Trans. Roy. Soc.* A **240**, 527.

DOBSON, F. W. 1971*a* *J. Fluid Mech.* **48**, 91.

DOBSON, F. W. 1971*b* *Boundary Layer Met.* **1**, 399.

ELLIOTT, J. A. 1972 *J. Fluid Mech.* **54**, 427.

GARRETT, C. & SMITH, J. 1976 *J. Phys. Ocean.* **6**, 925.

GENT, P. R. & TAYLOR, P. A. 1976 *J. Fluid Mech.* **77**, 105.

GENT, P. R. & TAYLOR, P. A. 1977 *Boundary Layer Met.* **11**, 65.

HASSELMANN, K. *et al.* 1973 *Dsch. Hydro. Z. Reihe* A(8°), no. 12.

KELLER, W. C. & WRIGHT, J. W. 1975 *Radio Sci.* **10**, 139.

LARSON, T. R. & WRIGHT, J. W. 1975 *J. Fluid Mech.* **70**, 417.

LONG, R. B. 1971 Ph.D. thesis, University of Miami, Florida.

LONGUET-HIGGINS, M. S. 1969*a* *Proc. Roy. Soc.* A **311**, 371.

LONGUET-HIGGINS, M. S. 1969*b* *Phys. Fluids* **12**, 737.

LONGUET-HIGGINS, M. S. 1977 *Deep-Sea Res.* (to appear).

MILES, J. W. 1957 *J. Fluid Mech.* **3**, 185.

MILES, J. W. 1959 *J. Fluid Mech.* **6**, 568.

MUNK, W. H., MILLER, G. R., SNODGRASS, F. E. & BARBER, N. F. 1963 *Phil. Trans. Roy Soc.* A **255**, 505.

PHILLIPS, O. M. 1966 *The Dynamics of the Upper Ocean.* Cambridge University Press.

SHEMDIN, O. H. 1969 *Coastal Engng Lab., Univ. Florida Tech. Rep.* no. 4.

SNODGRASS, F. E. *et al.* 1966 *Phil. Trans. Roy Soc.* A **259**, 431.

SNYDER, R. L. 1974 *J. Mar. Res.* **32**, 497.

SVERDRUP, H. U. & MUNK, W. H. 1947 *Wind, Sea and Swell. Theory of Relations for Forecasting.* Washington: U.S. Hydrog. Office, publ. no. 601.

TAYLOR, P. A., GENT, P. R. & KEEN, J. M. 1976 *Geophys. J. Roy. Astr. Soc.* **44**, 177.

TOWNSEND, A. A. 1972 *J. Fluid Mech.* **55**, 719.

VALENZUELA, G. R. 1976 *J. Fluid Mech.* **76**, 229.